ANL/RE/CP-94733

6th International Conference on Nuclear Engineering
ICONE-6
May 10-15, 1998

Paper #6079

DEFORMATION BEHAVIOR IN REACTOR PRESSURE VESSEL STEELS AS A CLUE TO UNDERSTANDING IRRADIATION HARDENING*

R.J. DiMelfi, D.E. Alexander and L.E. Rehn

Argonne National Laboratory, Argonne, IL 60439

March 8, 1998

R.J. DiMelfi
RE-208
Argonne National Laboratory
Argonne, IL 60439

(630) 252-3736
(630) 252-3075 (FAX)
dimelfi@anl.gov

*This work was performed under the auspices of the United States Department of Energy Technology Support Programs under Contract No. W-31-109-ENG-38.

DISCLAIMER

DISCLAIMER

Portions of this document may be illegible in electronic image products. Images are produced from the best available original document.

DEFORMATION BEHAVIOR IN REACTOR PRESSURE VESSEL STEELS AS A CLUE TO UNDERSTANDING IRRADIATION HARDENING

R.J. DiMelfi, D.E. Alexander and L.E. Rehn

R.J. DiMelfi
RE-208
Argonne National Laboratory
Argonne, IL 60439

(630) 252-3736
(630) 252-3075 (FAX)
dimelfi@anl.gov

Abstract

In this paper, we examine the post-yield true stress vs true strain behavior of irradiated pressure vessel steels and iron-based alloys to reveal differences in strain-hardening behavior associated with different irradiating particles (neutrons and electrons) and different alloy chemistry. It is important to understand the effects on mechanical properties caused by displacement producing radiation of nuclear reactor pressure steels. Critical embrittling effects, e.g. increases in the ductile-to-brittle-transition-temperature, are associated with irradiation-induced increases in yield strength. In addition, fatigue-life and loading-rate effects on fracture can be related to the post-irradiation strain-hardening behavior of the steels. All of these properties affect the expected service life of nuclear reactor pressure vessels. We address the characteristics of two general strengthening effects that we believe are relevant to the differing defect cluster characters produced by neutrons and electrons in four different alloys: two pressure vessel steels, A212B and A350; and two binary alloys, Fe-0.28 wt%Cu and Fe-0.74 wt%Ni.

Our results show that there are differences in the post-irradiation mechanical behavior for the two kinds of irradiation and that the differences are related both to differences in damage produced and alloy chemistry. We find that, while electron and neutron irradiations (at $T \leq 60°C$) of pressure vessel steels and binary iron-based model alloys produce similar increases in yield strength for the same dose level, they do not result in the same post-yield hardening behavior. For neutron irradiation, the true stress flow curves of the irradiated material can be made to superimpose on that of the unirradiated material, when the former are shifted appropriately along the strain axis. This behavior suggests that neutron irradiation hardening has the same effect as strain hardening for all of the materials analyzed. For electron irradiated steels, the post-yield hardening rate is clearly greater than that of the unirradiated material, and the flow curves cannot be made to superimpose. The binary iron-base model alloys studied here show a less pronounced difference in flow behavior for neutrons and electrons than exhibited by the steels, implicating the effect of alloy chemistry. Our results are analyzed in the context of classical theories dealing with the interaction between the deformation microstructure, i.e. glide dislocations, and irradiation-produced defects. Our findings provide clues about the way different alloy constituents interact with the different kinds of irradiation damage to strengthen the material differently.

Introduction

Irradiation embrittlement of nuclear reactor pressure vessel steels continues to be of great importance to the energy research community (Gold et al., 1995). This is particularly true as life prediction of aging reactors and extension of their licenses become increasingly at issue (Code of Federal Regulations, 1996). Along with this increase in interest comes an array of promising experimental and theoretical tools that allow radiation effects and their consequences to be more carefully studied and better understood than in the past. These involve the ability to perform more carefully controlled irradiation experiments, the existence of higher resolution tools for both direct (e.g., electron microscopy) and indirect (e.g., small angle scattering) observation of irradiation-produced defects, and advances in atomistic computer simulations of irradiation effects and of intrinsic and extrinsic defect interactions. However, embrittlement is in fact a mechanical property, and the mechanical behavior of the material can provide important clues as to the root causes of embrittlement and serve as a guide as to what to look for and how to model it. One cause of embrittlement is irradiation hardening. In this note, we use the post-yield deformation behavior of irradiated materials as a probe into the phenomenon of irradiation hardening and embrittlement.

One measure of irradiation embrittlement in steels is the shift to higher temperatures of the ductile-to-brittle-transition-temperature (DBTT) after exposure to displacement-producing radiation. In this class of alloys, the yield stress increases with decreasing temperature, while the brittle fracture stress is essentially temperature independent. As the temperature is lowered, the yield stress increases relative to the brittle fracture stress and, at some low temperature, it can reach a level above the brittle fracture stress. Above this transition temperature, the steel when loaded will yield first and deform plastically before fracture, exhibiting a relatively high toughness, but below the DBTT, the steel will fracture without plastic flow and, hence, in a brittle manner. For engineering application, the steel is chosen so that the DBTT is well below any operating temperature. Irradiation of the steel can raise its DBTT by as much as 200°C (Pachur, 1981), bringing it into the operating temperature regime.

It is widely accepted that the shift to higher transition temperature after irradiation is the result of an overall increase in the yield stress, causing the above process to occur at a higher temperature. This overall increase in yield stress is caused by the interaction between glide dislocations and irradiation-produced point defect clusters. These clusters can be intrinsic in nature (made up of vacancies or self-interstitials only) or extrinsic (involving both solute species and intrinsic point defects). Because of the direct connection between yield stress and DBTT, and because tensile tests are more standardized and reproducible than fracture tests, much of the work in this area involves studies of the effects of displacement-producing irradiation on the yield strength measured in a tensile test. However, while yield strength changes may be directly related to changes in DBTT, the post-yield flow behavior can provide insight into the nature of irradiation-produced defects and their interaction with glide dislocations. We suggest here that important clues about the nature of irradiation hardening and embrittlement can be obtained from post-yield flow behavior. This information can be helpful in the study of reactor pressure vessel lifetime issues.

Recently, Alexander and Rehn (1994) and Alexander et al. (1996) have done work that reveals some important effects associated with gamma irradiation of reactor pressure vessel steels. The damage produced by gammas is almost entirely caused by high-energy Compton electrons and pair-produced electrons and positrons. Therefore, these authors studied the effects of gamma irradiation in carefully controlled experiments using direct electron irradiation. They studied both conventional pressure vessel steels and simple iron-base alloys that were designed to model these steels and to allow a focus on specific defect-solute interactions. Alloy compositions are shown in Table I. One of their findings was a notable similarity between the strengthening effects of gammas (electrons) and those produced by neutrons when compared on a displacements per atom (dpa) basis after irradiations at low temperatures ($T \leq 60°C$). This observation is

Table I. Elemental Compositions of Alloys in Weight Percent

Element	A212B	A350	Fe-0.28 Cu	Fe-0.74Ni
C	0.26	0.18	0.013	0.01
Al	0.07	0.08	0.007	<0.005
Co	0.015	0.03		
Cr	0.075	0.090		
Cu	0.15	0.11	0.28	<0.005
Mn	0.85	0.55	0.013	0.017
Mo	0.02	0.03		
Nb	<0.001	<0.001		
Ni	0.20[a]	3.3	0.012	0.74
Si	0.29	0.29		
Sn	0.02	0.02		
Ti	0.01	<0.001		
V	0.0005	0.001		
W	<0.005	<0.005		
Zr	<0.001	<0.001		
P	0.006	0.01	0.004	0.003
S	0.04	0.02		
As	0.007	0.01		
B	<0.0005	<0.0005		
N	0.0060	0.0090		
O	0.0024	0.0027		

[a] Believed to be high; independent analysis at another laboratory showed 0.09 wt. %

consistent with the apparent additivity of the effects of gamma and neutron irradiation resulting in the "accelerated" embrittlement of the High Flux Isotope Reactor (HFIR) at Oak Ridge National Laboratory (Farrell et al., 1994 and Remec et al., 1994). This similarity and apparent additivity of embrittling effects observed after low temperature irradiations are remarkable in view of the considerable differences in the kinds of damage produced by neutrons and electrons. The authors found this phenomenon explainable in terms of a reaction-rate theory model of defect production and clustering (Alexander et al.,1996; Stoller, 1993a; and Stoller, 1993b). Their observations are significant for a number of reasons. Certain advanced-reactor designs are such that the gamma-irradiation damage at the reactor pressure vessel is a substantial fraction of the neutron-irradiation damage. This makes it important in these cases to understand the way gamma damage accumulates and embrittles the steel, both alone and in relation to neutron effects. Also, the scientific understanding of the relationship between electron and neutron irradiation effects that can be revealed by such studies may make it possible to study irradiation embrittlement in a fundamental way through carefully-controlled electron irradiation experiments.

Nonetheless, it is surprising and provocative to find that electrons and neutrons affect the yield strength in very much the same way. Because of the likely difference in damage produced by these different kinds of irradiation, other mechanical properties may be affected differently, and these differences can serve to enlighten us further about radiation effects in general. An examination of these differences can also help us understand how the effect on the yield stress can be similar after both kinds of irradiation. We briefly explore these issues in the remainder of this note.

Analysis

Background

In order to gain more insight regarding the effects of irradiation on mechanical properties, we examine the entire true-stress flow behavior of irradiated materials. The yield strength is increased by irradiation when the displacement damage produces an additional distribution of barriers to dislocation glide, increasing the initial stress required for plastic flow. As has been stated, these new barriers (defect clusters) can be intrinsic or extrinsic in nature. Depending on their character and the way they interact with glide dislocations, these irradiation-produced barriers can affect the post-yield flow behavior in two different ways, even if they increase the yield stress by the same amount. We address here the general characteristics of these two strengthening effects, which we believe are each reflective of the kind of defect clusters produced.

In one strengthening mechanism, the defect clusters effectively increase the yield stress in the same way that strain-hardening an unirradiated sample does. In this case, when the yield stress value of the irradiated sample is shifted along the strain axis and placed on the same flow curve as that of the unirradiated sample, plastic flow of the irradiated sample continues along this same true-stress true-strain curve. This is illustrated schematically in Fig.1. If this kind of irradiation strengthening occurs, the irradiated sample and the unirradiated sample will exhibit the same true stress at ultimate strength ($\sigma_U^I = \sigma_U^N$). (Properties for unirradiated (non-irradiated) materials are noted by the superscript N and irradiated materials by I.) This phenomenon has been observed at all fluence levels for the case of type 316 stainless steel, neutron-irradiated over a wide range of fluence levels (DiMelfi and Kramer, 1980). However, in such cases the engineering ultimate tensile stress (UTS) of the irradiated sample (UTS^I) will have a higher value than that of the unirradiated sample (UTS^N), when comparing engineering curves. This is because the unirradiated sample will elongate more before reaching the true stress at ultimate than the irradiated sample does to reach the same true stress level. The increase in UTS^I with increasing dose can be misleading in this case because the true strength at ultimate is the same for both. After yielding, the two materials obey the same flow law, but the true-stress vs. true-strain curve for the irradiated material is shifted along the strain axis to a higher value of strain. The irradiation embrittlement in this case is a reflection of the loss in tensile ductility resulting from the material

being brought closer to the point of plastic instability by irradiation hardening. For this type of strengthening, the tensile sample fails earlier with increasingly less uniform elongation with increasing dose.

Another way that irradiation strengthening can occur is when the interaction between irradiation-produced defect clusters and glide dislocations is such that the irradiated sample not only yields at a higher stress than the unirradiated sample, but flow continues at a higher hardening rate after yielding, as illustrated schematically in Fig. 2. For this kind of strengthening, not only will the UTS be greater for the irradiated material, but so will the true stress at ultimate, σ_U. This suggests that the nature of the irradiation-produced barriers to plastic flow is different from that discussed in the first case. The two differing mechanical responses are, in essence, fingerprints of differing defect characteristics.

Fig. 1. Schematic true stress curves representing flow behavior in an unirradiated sample (solid line) and an irradiated sample for the case where irradiation hardening behaves like strain hardening. After the curve for the irradiated sample is shifted to the right along the strain axis so that its yield stress falls on the unirradiated-sample curve, the two curves essentially coincide and pass through the same σ_U value.

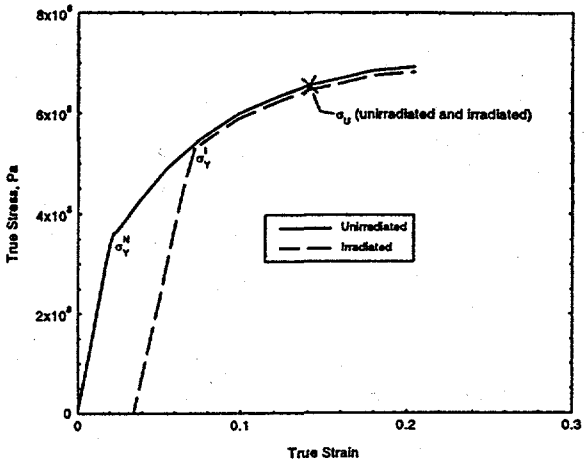

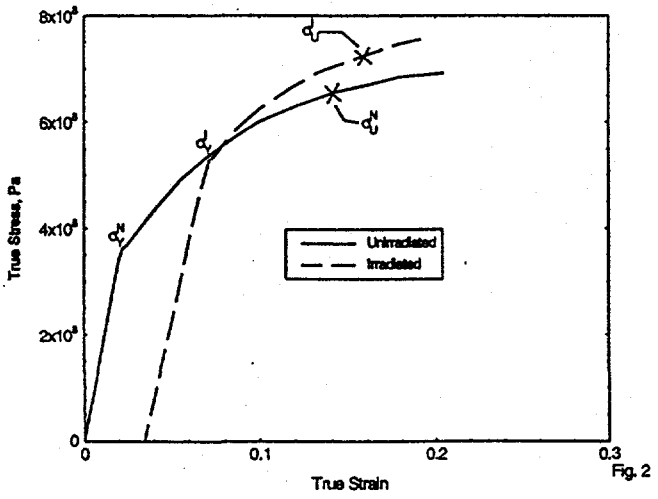

Fig. 2

Fig. 2. Schematic true stress curves representing flow behavior in an unirradiated sample (solid line) and an irradiated sample. In this case irradiation hardening is such that post-yield flow continues at a higher strain-hardening rate than that of the unirradiated-sample after the irradiated-sample curve is shifted so that its yield stress falls on the unirradiated-sample curve. The true stress at ultimate for the irradiated sample σ_U^I is greater than that for the unirradiated sample σ_U^N.

As outlined above, the plastic flow behavior of irradiated materials can provide important information about the nature of defects produced by different kinds of irradiation in alloys of differing chemistry. This information will allow us to understand better the different embrittling effects caused by different kinds of irradiation and will help to make better use of the results of electron irradiation experiments as simulations of gamma and neutron irradiation. Also, these different irradiation-hardening effects can have important consequences with regard to pressure vessel life prediction. Even if the changes in yield stress, and hence the changes in DBTT, are quite similar at the same dpa level for neutron and electron irradiation as mentioned in the previous section, this is only one mechanical property issue. The DBTT is loading-rate dependent, and changes in the hardening rate for different irradiating species may affect this dependence and thereby influence brittle fracture. The presence or lack of a yield drop, or its prominence, after different kinds of irradiation may affect the conditions of fracture. Also, while the true stress at ultimate is unrelated to the DBTT, it is intimately related to fatigue life, and the extent to which σ_U is changed by irradiation will affect the fatigue life of a component. Finally, differing solute species from one alloy to another may interact differently with the same kind of nascent irradiation damage, affecting the kinds of defect clusters formed.

Data Analysis

Raw tensile data on the irradiated alloys studied in this paper were provided by Farrell (1996). These data were obtained from miniature (ASTM SS-3) tensile specimens, and sample extension was extracted from the machine cross head displacement. In the present analysis, we assumed that this reported extension occurred only the gauge section of the sample. Possible consequences of this assumption are discussed later. Tabulated data on irradiated pressure-vessel steels reported in Ref. 5 (Alexander, et al., 1996) suggest that **neutron** irradiation of these steels produces the first kind of behavior discussed above. Throughout this analysis, the true stress is determined from the reported uniform elongation and the assumption of constant volume during plastic flow, and the true strain is determined only to the point of maximum load. Figure 3 shows the true-stress true-plastic-strain flow curves extracted from the raw data for A212B, neutron irradiated to a range of damage levels expressed in displacements per atom (dpa). Figure 3a shows the flow behavior for this material for the range of irradiation conditions with each curve referenced to zero plastic strain in each case. Figure 3b shows the same curves for irradiated material shifted horizontally along the strain axis so that their yield stress lies on the unirradiated curve. When this is done, the flow curves for irradiated material superimpose on the curve for unirradiated material. In this case, the *true* stress at ultimate is essentially the same for both unirradiated samples and samples irradiated over the range of doses, where hardening is below the true stress at ultimate. However, at the highest damage levels, where hardening is beyond this stress level, failure occurs just after yielding with no uniform elongation. At these damage levels, the materials yields beyond the point of plastic instability. Nonetheless, the yield strength for these samples lies on the extension of the stress-strain curve for unirradiated material. This behavior is consistent with that displayed by true-stress flow curves of neutron irradiated type 316 stainless steel (DiMelfi and Kramer, 1980)and several advanced ferritic and austenitic stainless steels (Goshchitskii and Sagaradze, 1995) similarly exposed. Early data (Wilson, 1958) on one of these very same pressure vessel steels (A212B) exhibit essentially the same behavior when the UTS is analyzed in this way. Figure 4 shows similar behavior for A350 and the Fe-Cu and Fe-Ni binary alloys after the curves for irradiated material have been shifted appropriately along the strain axis.

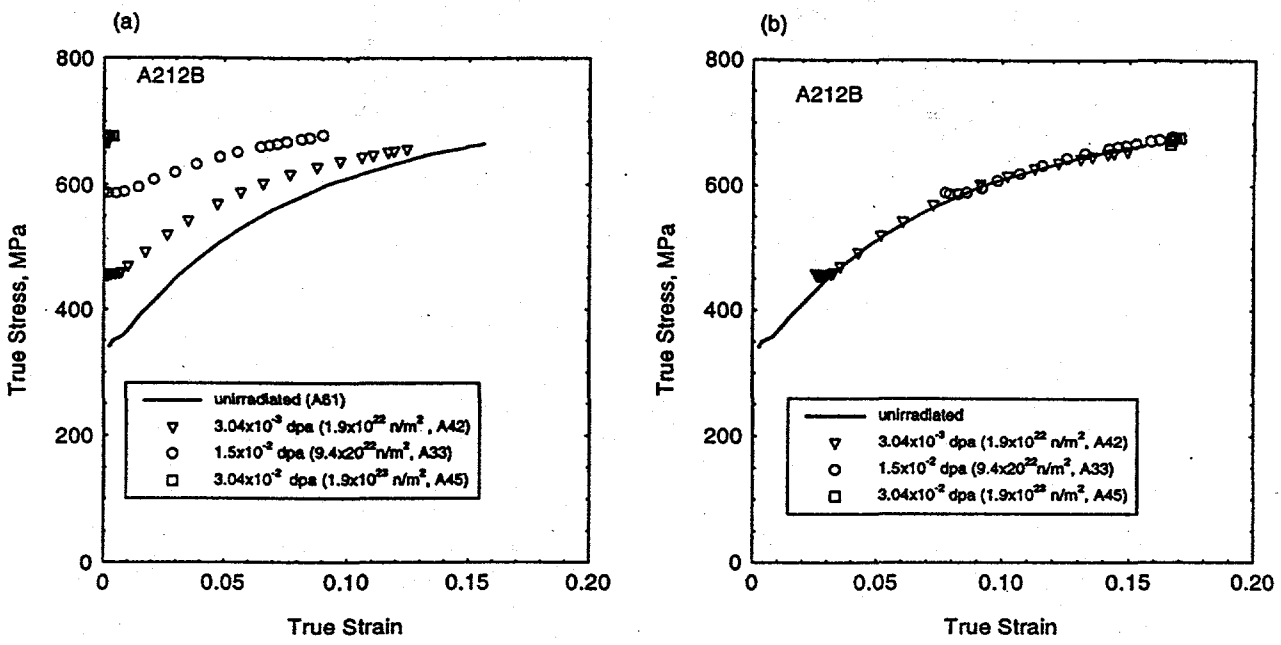

Fig. 3. The true stress flow curves for neutron irradiated (T≤ 60 °C) pressure vessel steel A212B to the indicated fluence and corresponding damage levels is shown. In 3(a) the flow curves are left unshifted and referenced to zero plastic strain in each case. In 3 (b) the curves are shifted along the strain axis so that their yield stress falls on the flow curve for unirradiated material.

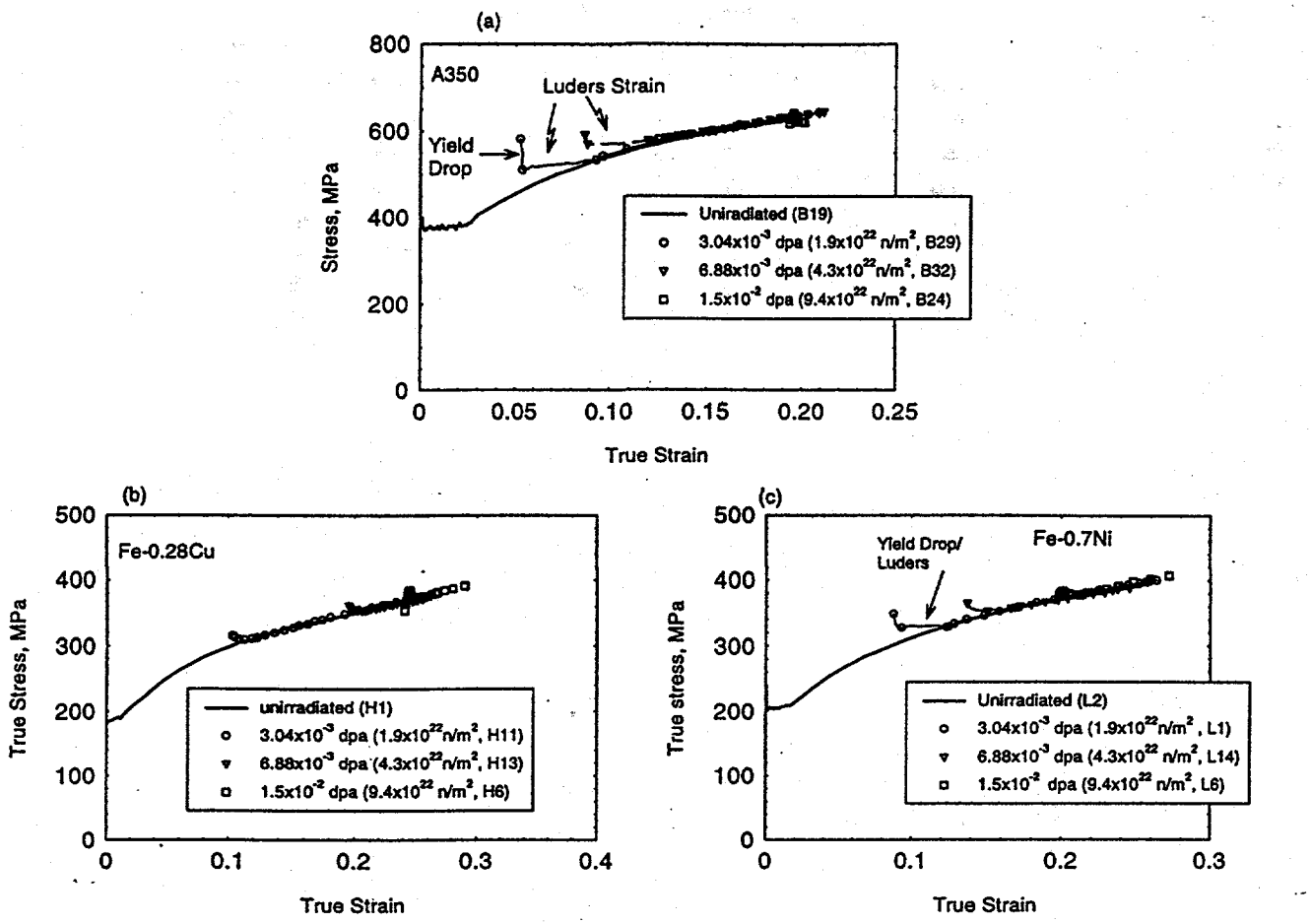

Fig. 4. The true stress flow curves for neutron irradiated (T≤ 60 °C) pressure vessel steel A350 (a), Fe-0.28 Cu (b) and Fe-0.74 Ni © to the indicated fluence and corresponding damage levels is shown. The flow curves are shifted along the strain axis so that the point where uniform flow begins in each case (after Lüders-strain is complete) coincides with the flow curve for unirradiated material.

Electron irradiation of the same pressure-vessel steels (Alexander et al., 1996) produces the second kind of behavior discussed above. The true-stress flow curves for the electron irradiated A212B samples are shown Fig.5. In Fig. 5a, the flow curves are shown not shifted, i.e. referenced to zero plastic strain in each case. In Fig. 5b, these curves are shifted horizontally to the right along the strain axis to points where their yield stress values intersect the same stress level on the unirradiated-sample flow curve. Unlike in the case of neutrons, after yielding, the flow curves for irradiated A212B continue at higher hardening rates than that of the unirradiated material. This is so, even though, as indicated previously, the yield stress changes after irradiation are quite similar at the same damage level for both kinds of irradiation (for irradiations at $T \leq 60°C$). As with the increases in yield strength, the increases in hardening rate at a given stress are systematic with increasing dose.

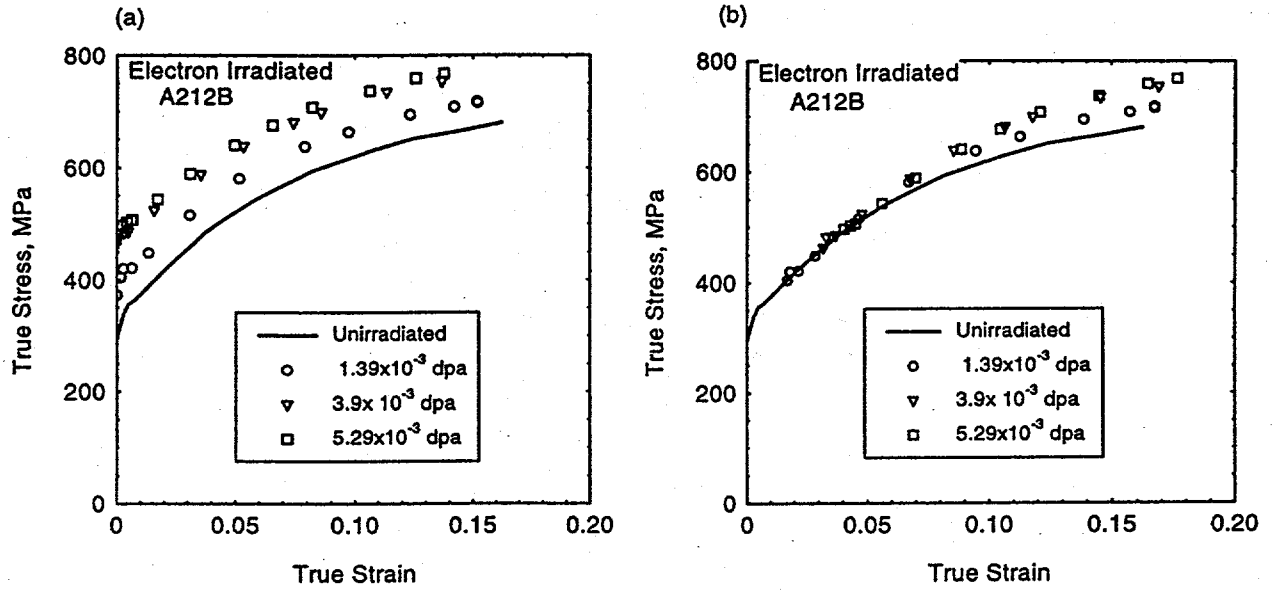

Fig. 5. The true stress flow curves for electron irradiated (35 °C≤ T≤ 60 °C) pressure vessel steel A212B to the indicated damage levels is shown. In 5(a) the flow curves are left unshifted and referenced to zero plastic strain in each case. In 5 (b) the curves are shifted along the strain axis so that their yield stress falls on the flow curve for unirradiated material.

A similar effect is shown in Fig. 6 for A350, where the curves for irradiated material are shifted along the strain axis as described above. The true-stress flow curves for electron irradiated samples of Fe-0.28Cu and Fe-0.74Ni are shown in Fig.7. It is seen in this figure that, for these alloys, the post-yield hardening rate of the electron-irradiated materials is not as clearly different from that of unirradiated materials as it is in the case of the steels. Therefore, for the binary alloys, the post-yield strain-hardening behavior is not very different after irradiation hardening by either electrons or neutrons. These results imply that the putative solute-point defect interaction/clustering effect that causes the distinct difference between electron and neutron irradiation-strengthening in pressure vessel steels (cf. next section) is less prominent in these model alloys.

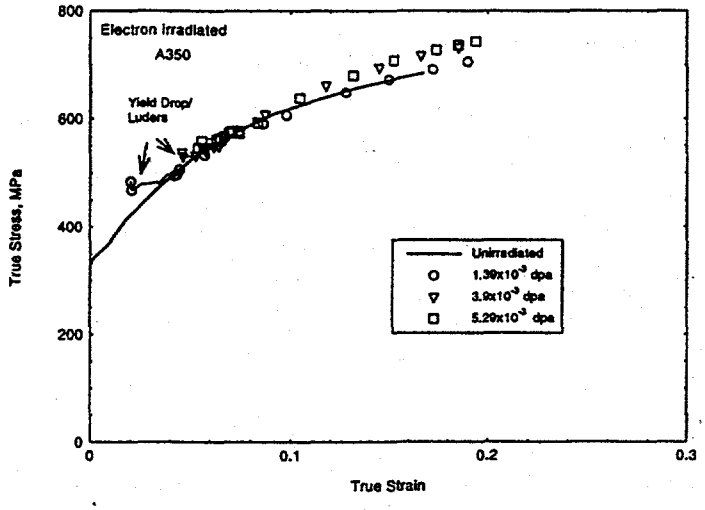

Fig. 6. The true stress flow curves for electron irradiated (35 °C≤ T≤ 60 °C) pressure vessel steel A350 to the indicated damage levels is shown. The curves are shifted along the strain axis so that their yield stress (after yield drop and/or Lüders strain is complete) falls on the flow curve for unirradiated material.

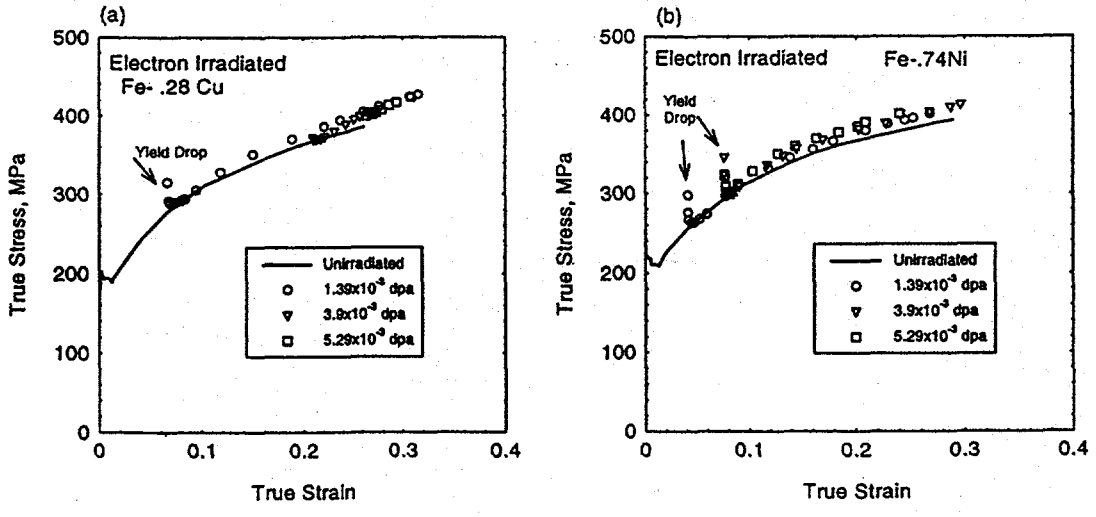

Fig. 7. The true stress flow curves for electron irradiated (35 °C≤ T≤ 60 °C) Fe-0.28 Cu (a) and Fe-0.74 Ni (b) to the indicated damage levels is shown. The curves are shifted along the strain axis so that their yield stress (after yield drop and/or Lüders strain is complete) falls on the flow curve for unirradiated material.

Results and Discussion

The collection of results for both steels and model alloys displayed above indicates that irradiation particle and alloy chemistry are both important to producing a particular kind of strengthening phenomenon. There are clearly substantial differences in the primary damage states produced by electron versus fast neutron irradiation. Fast neutrons tend to produce cascades containing a high density of intrinsic point defects in close proximity to one another and this proximity results in considerable in-cascade clustering and annihilation. In contrast, the low energy recoils generated by electron irradiation tend to produce isolated point defects with minimal clustering during the displacement process. One might expect that the cascade damage caused by neutron irradiation would produce defect clusters that are different in nature from those produced by the more uniformly distributed electron damage, and that this would result in different strengthening effects. However, it appears that for the low temperature tests discussed here the yield stress increases are quite similar for both kinds of irradiation to the same dose level (dpa) for all the materials tested. In the previously mentioned work (Alexander et al.,1996; Stoller, 1993a; and Stoller, 1993b), rate theory modeling in pure Fe demonstrated that, despite the large differences in defect production, the microstructures which evolve, whether formed by electron or neutron irradiation, could result in essentially the same yield strength increase.

The difference in post-yield flow behavior for electron and neutron irradiation is clearly apparent in the steels and less so in the model alloys for irradiations in the low temperature range ($T \leq 60°C$) studied here. One way to understand this behavior is to imagine that the increases in yield strength are determined by the required for glide dislocation s to pass the irradiation-produced defect clusters, whatever their nature. This approach and variations on it are what is usually done in analyses of this phenomenon (Odette, in press). These clusters must have more or less the same number density for the two kinds of irradiation in order for them to have the same effect on the yield strength. However, the difference in post-yield flow behavior observed in the irradiated steels suggests inherent differences in character between those clusters produced by electrons versus those produced by neutrons. The fact that flow behavior differences are not observed in the two model alloys suggests that alloy chemistry is also involved in producing microstructural and mechanical behavior differences in the irradiated steels.

The exact nature of the defect clusters comprising the irradiated steel microstructure cannot be definitively determined by the current analysis; however, important clues are present. First, the observation that the flow curves of neutron irradiated steels exhibit, after shifting along the strain axis, a flow behavior similar to unirradiated steels suggests that the defect clusters produced in this case cause a hardening behavior similar to strain hardening. Second, the increased post-yield hardening rate observed for electron irradiated steels suggests that the resulting defect clusters are such that they alter the dislocation multiplication rate after yielding beyond that which can be attributed to normal strain hardening in unirradiated material. Third, the fact that the defect clusters, which produce an increased strain hardening rate, form during electron irradiation and not during neutron irradiation of the steels indicates that both the primary damage state and the subsequent interaction of defects with key alloy element(s) in the steels figure importantly in the formation of these defect clusters. Fourth, the more pronounced increase in post-yield hardening rate observed in the electron irradiated steels than in electron-irradiated model alloys implies that alloying element(s), other than Cu or Ni, present in the steels influence the formation of such defect clusters.

We also wish to point out that the different defect cluster character implied by the different flow behavior for the two kinds of irradiation, particularly in the steels, may also result in different yield point and yield drop phenomena. These differences can also lead to differences in the nature of certain aspects of irradiation embrittlement.

There can be difficulties in extracting reliable values of uniform elongation from the raw tensile data

provided by Farrell (1996). The samples were small, with a one-inch overall length and a gauge length of only 0.3 in., and the reported sample extensions were obtained from the cross head displacement rather than from the gauge section alone. The concern is that, because of sample size, extensions outside the sample gauge section would make an inordinate contribution to the presumed uniform extension attributed to the gauge section, which we ultimately used to determine the true stress. This could be a particular problem in the electron irradiated samples, where, in some cases, irradiation hardening did not extend much beyond the gauge section leaving the shoulder section softer and more likely to contribute spurious strains. Load was applied to these samples through circular pinholes in the shoulder region of the dogbone shaped samples. We measured the eccentricity of the pinholes of the deformed electron-irradiated samples as well as the overall dimensional changes of the shoulder region, and found no indication of deformation large enough to give false inferences regarding uniform elongation in the gauge section. This suggests that the sample design provides sufficient bulk to the shoulder region to keep it from deforming significantly, even with an irradiation hardened gauge section. As a further precaution, we recalculated the true stress of the electron-irradiated samples assuming that 33% of the uniform elongation (i.e. 5% out of 15% uniform elongation) was attributable to extension outside the gauge section. The calculated true-stress values decrease by only about 4%. More importantly, even with this recalculation, the post-yield hardening rate of the electron irradiated steels was higher than that of the unirradiated material and the behavior was still prominently different from that exhibited by neutron irradiated material in the same manner described in this paper. We should also note that, while many samples, both unirradiated and irradiated with neutrons and electrons, exhibited yield point phenomena and Lüders deformation, none of the Lüders strains observed in the tensile data was large enough to affect our results, and, after the Lüders deformation was completed, uniform flow and hardening in the gauge section proceeded as shown in the graphs in this paper.

Summary and Conclusions

In this paper, we have shown that there are differences in the post-irradiation mechanical behavior for the two kinds of irradiation and that the differences are related both to differences in damage produced and alloy chemistry. We have found that electron and neutron irradiations (at $T \leq 60\,^{\circ}C$) of pressure vessel steels and binary iron-based model alloys, while they produce the same increases in yield strength for the same dose level, do not result in the same post-yield hardening behavior. This is revealed through an examination of the true-stress flow curves for these materials. For neutron irradiation, the true stress flow curves of the irradiated material superimpose on that of the unirradiated material, when the former are shifted along the strain axis. The post-yield hardening rate is the same as that of the unirradiated material deformed to the same stress level, as is observed in other steels (DiMelfi and Kramer, 1980; Goshchitskii and Sagaradze, 1995). This behavior suggests that neutron irradiation hardening has the same effect as strain hardening, and the loss of ductility (embrittlement) is caused by material being brought closer to the point of plastic instability (or beyond it) with increasing irradiation dose levels. For electron irradiated steels, the post-yield hardening rate is clearly greater than that of the unirradiated material.

These results can be interpreted both in terms of the different kinds of damage produced by neutrons and electrons, cascades versus uniformly dispersed defects, respectively, and in terms of steel chemistry. We suggest that, in the case of electron damage, alloying element(s) in the steels may play an important role in the formation of defect clusters that not only increase the strength of the material to produce a higher yield stress, but also alter the post-yield dislocation multiplication rate beyond that which would exist from just strain hardening. Their presence would result in a higher hardening rate during post-yield deformation of electron irradiated steels than would result from simply strain hardening or neutron irradiating to achieve the same yield strength. Also, it is possible that the presence of these electron irradiation-produced clusters may result in different yield-point phenomena in a tensile test than those produced by neutron irradiation, which only

produces strengthening similar to strain hardening in these steels. However, observing such differences depends on the sensitivity of the tensile test.

The binary iron-base model alloys studied here show a less pronounced difference in flow behavior for neutrons and electrons. This difference in behavior from the steels can provide insight into these irradiation effects in general and suggest future work in this area. If it is assumed that the binary alloys are lacking those element(s) in the steels that interact with the electron damage state to increase the post-yield hardening rate, then the observation of similar yield stress increases implies that the two kinds of irradiation produce roughly the same defect cluster density whether or not that solute is present. The presence of those element(s) in the steels serves mainly to change the nature and stability of the particular defect cluster in question.

Acknowledgments

The authors gratefully acknowledge Dr. Ken Farrell for apprising us of important issues regarding the tensile testing of irradiated small specimens and for providing us with the raw tensile data he obtained, which was used in our analysis. This work was performed under the auspices of the United States Department of Energy and was supported by the US Department of Energy Technology Support Programs and BES-Materials Sciences under Contract No. W-31-109-ENG-38.

References

1. R.E. Gold, A.R. McIlree and S.M. Breuemmer, editors, *Proceedings of the Seventh International Symposium on Environmental Degradation of Materials in Nuclear Power Systems - Water Reactors*, NACE International, Houston TX, 1995.
2. Code of Federal Regulations, "Requirements for Renewal of Operating Licenses for Nuclear Power Plants" , Title 10, Part 54, Sections 1-43, revised Jan. 1, 1996.
3. D. Pachur, in *Proceedings of the Tenth International Symposium on Effects if Radiation on Materials*, eds. David Kramer, H.R. Brager and J.S. Perrin, ASTM STP 725, Philadelphia PA, 1981, pp. 5-19.
4. D.E. Alexander and L.E. Rehn, J. Nucl. Mater. **217**, 213-216 (1994).
5. D. E. Alexander, L.E. Rehn, K. Farrell, and R.E. Stoller, J. Nucl. Mater. **228**, 68-76 (1996).
6. K. Farrell, S.T. Mahmood, R.E. Stoller and L.K. Mansur, J. Nucl. Mater. **210**, 268-281 (1994).
7. I. Remec, J.A. Wang, F.R. Kam and K. Farrell, J. Nucl. Mater. **217**, 258-269 (1994).
8. R.E. Stoller (1993a), in *Effects if Radiation on Materials*, eds. A.S. Kumar, D.S. Gelles, R.K. Nanstad and E.A. Little, ASTM STP 1175, Philadelphia PA, 1993, pp. 394-423.
9. R.E. Stoller (1993b), in *Proceedings of the Sixth International Symposium on Environmental Degradation of Materials in Nuclear Power Systems - Water Reactors*, eds. R.E. Gold and E. Simonen, TMS, Warrendale, PA, 1993, pp.747-754.
10. R.J. DiMelfi and J.M. Kramer, J. Nucl. Mater. **89** ,338-346 (1980).
11. K. Farrell, private communication, 1996
12. B. Goshchitskii and V. Sagaradze, private communication under U.S. Russian Agreement #942492402, *Report on the Development of Radiation Resistant Alloys*, December, 1995, Yekaterindurg, Russia.
13. J.C. Wilson, in *2nd United Nations Conference on the Peaceful Uses of Atomic Energy*, Geneva, Switzerland, **5**: 431 (1958); and reported in *Radiation Effects on Toughness of Ferritic Steels for Reactor Vessels, An AEC Monograph*, L.P. Trudeau, Rowman Littlefield, Inc., New York, 1964, p. 53.
14. G. R. Odette, "Neutron Irradiation Effects in Reactor Pressure Vessel Steels and Weldments", IAEA Technical Report Series, M. Davies, ed., Vienna (in press).

Figure Captions

Figure 1. Schematic true stress curves representing flow behavior in an unirradiated sample (solid line) and an irradiated sample for the case where irradiation hardening behaves like strain hardening. After the curve for the irradiated sample is shifted to the right along the strain axis so that its yield stress falls on the unirradiated-sample curve, the two curves essentially coincide and pass through the same σ_U value.

Figure 2. Schematic true stress curves representing flow behavior in an unirradiated sample (solid line) and an irradiated sample. In this case irradiation hardening is such that post-yield flow continues at a higher strain-hardening rate than that of the unirradiated-sample after the irradiated-sample curve is shifted so that its yield stress falls on the unirradiated-sample curve. The true stress at ultimate for the irradiated sample σ_U^I is greater than that for the unirradiated sample σ_U^N.

Figure 3. The true stress flow curves for neutron irradiated ($T \leq 60°C$) pressure vessel steel A212B to the indicated fluence and corresponding damage levels is shown. In 3(a) the flow curves are left unshifted and referenced to zero plastic strain in each case. In 3 (b) the curves are shifted along the strain axis so that their yield stress falls on the flow curve for unirradiated material.

Figure 4. The true stress flow curves for neutron irradiated ($T \leq 60°C$) pressure vessel steel A350 (a), Fe-0.28 Cu (b) and Fe-0.74 Ni © to the indicated fluence and corresponding damage levels is shown. The flow curves are shifted along the strain axis so that the point where uniform flow begins in each case (after Lüders strain is complete) coincides with the flow curve for unirradiated material.

Figure 5. The true stress flow curves for electron irradiated ($35°C \leq T \leq 60°C$) pressure vessel steel A212B to the indicated damage levels is shown. In 5(a) the flow curves are left unshifted and referenced to zero plastic strain in each case. In 5 (b) the curves are shifted along the strain axis so that their yield stress falls on the flow curve for unirradiated material.

Figure 6. The true stress flow curves for electron irradiated ($35°C \leq T \leq 60°C$) pressure vessel steel A350 to the indicated damage levels is shown. The curves are shifted along the strain axis so that their yield stress (after yield drop and/or Lüders strain is complete) falls on the flow curve for unirradiated material.

Figure 7. The true stress flow curves for electron irradiated ($35°C \leq T \leq 60°C$) Fe-0.28 Cu (a) and Fe-0.74 Ni (b) to the indicated damage levels is shown. The curves are shifted along the strain axis so that their yield stress (after yield drop and/or Lüders strain is complete) falls on the flow curve for unirradiated material.